

Booster Neutrino Flux Prediction at MicroBooNE

MicroBooNE Collaboration

July 6, 2018

MICROBOONE-NOTE-1031-PUB

Abstract

The primary source of neutrinos for the MicroBooNE experiment is Fermilab's Booster Neutrino Beamline. The beamline uses 8 GeV protons from the Booster accelerator steered onto a beryllium target. The secondaries are focused by a magnetic horn down a 50m long decay pipe. Decays of these secondaries give rise to a neutrino beam. We use the beamline simulation and techniques previously developed by the MiniBooNE collaboration to calculate the neutrino flux and estimate systematic uncertainties at the MicroBooNE detector location.

1 Introduction

The MicroBooNE detector is located in the same Booster Neutrino Beamline (BNB) as the MiniBooNE detector at a baseline of 468.5m. After many years of operation, MiniBooNE developed a well constrained beamline simulation based on the GEANT4 framework [1] as well as techniques to handle systematic uncertainties [2]. Following the original publication of neutrino flux predictions in the BNB, MiniBooNE updated the simulation to include the SciBooNE measurement of $p + Be \rightarrow K^+$ production in the BNB [5, 6]. The update changed the flux prediction, and provided a better constraint on kaons produced in BNB. Furthermore, MiniBooNE also developed a better technique for evaluating π^+ and π^- production uncertainties by using the HARP pion production data directly rather than a fit parametrization. This technique allowed the HARP measurement uncertainties to be more properly propagated to the calculated neutrino flux. The data-based HARP uncertainties were used to produce all of the MiniBooNE oscillation and cross section results (cf. [3, 4]).

We adapted these tools and techniques to calculate neutrino flux and systematic uncertainties at the MicroBooNE detector location, and reimplemented them into the LArSoft framework [7] used to analyze MicroBooNE data.

The calculations shown here were done for the neutrino mode configuration in which the horn is pulsed with +174 kA.

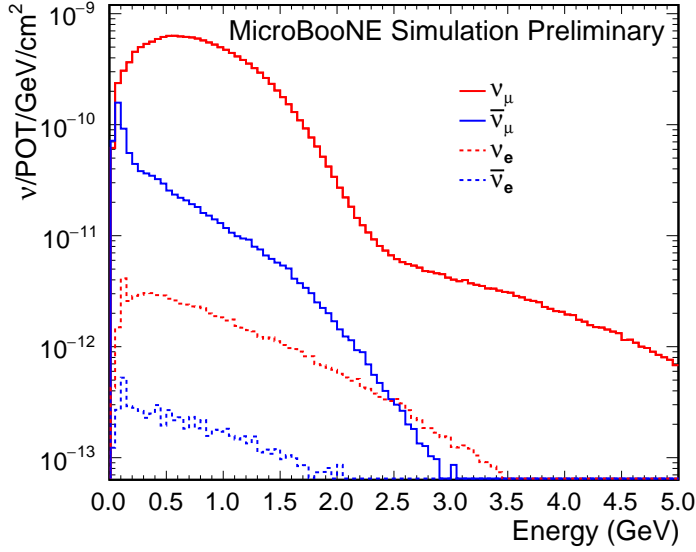


Figure 1: The absolute neutrino flux prediction through the MicroBooNE detector as calculated by the beam simulation. Shown is the flux for ν_μ , $\bar{\nu}_\mu$, ν_e , and $\bar{\nu}_e$ averaged through the TPC volume with dimensions $2.56\text{m} \times 2.33\text{m} \times 10.37\text{m}$.

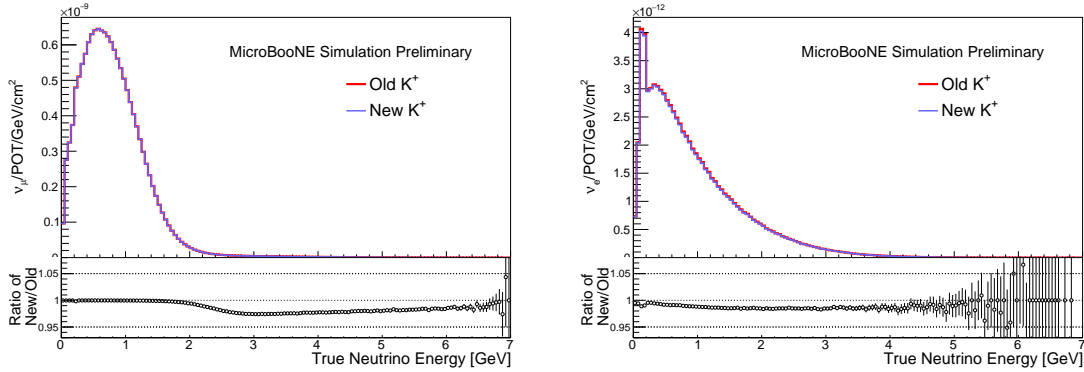


Figure 2: The ν_μ (left) and ν_e (right) neutrino flux just upstream of the MicroBooNE detector. Shown is the comparison of flux constrained by global fit to K^+ production data (old) to the one that additionally includes SciBooNE data [6] (new).

2 Neutrino Flux Calculation

Figure 1 shows the predicted neutrino flux averaged through the MicroBooNE detector TPC volume. This is the absolute flux as generated by the simulation. No scaling factors are needed or applied.

Figure 2 shows the effect on the neutrino flux when SciBooNE data [5] is included in the global fit of K^+ production data [6]. Note that the flux shown in the figure was calculated upstream of MicroBooNE detector, and not averaged through TPC volume as in Figure 1.

3 Systematic uncertainties

The flux uncertainties were evaluated for the same set of systematics as considered in Ref. [2]. The uncertainties can be split into two categories.

- Hadron production: π^+ , π^- , K^+ , K^- , and K_L^0
- Non-hadron production: mismodeling of horn current distribution, horn current miscalibration, pion and nucleon total, inelastic, and quasielastic scattering cross-sections on beryllium and aluminum

Additionally we assign a 2% normalization uncertainty due to uncertainties in proton delivery. This includes the beam intensity measurement uncertainty, and the uncertainty in number of protons actually hitting the target. Beamline instrumentation is used to monitor the beam on spill-by-spill basis. The beam intensity is monitored using two beam toroids with a precision at the 1% level. The beam position at the target is derived from several horizontal and vertical beam position monitors upstream of the target. The profile of the beam is monitored using horizontal and vertical multiwire monitors. Beam quality cuts are used to eliminate data where any significant fraction of the beam misses the target keeping the total proton delivery uncertainty below 2%.

The exact same $\pm 1\sigma$ variations of the underlying parameters were applied as in Ref. [2] except for charged pion production and K^+ production where subsequent improvements were adapted, as described above. With these updates the underlying uncertainties are the same as in recent MiniBooNE analyses (for example as in Ref. [4]).

Figure 3 shows the correlation matrices for muon and electron neutrinos calculated after including all of the systematic uncertainties. Figure 4 shows the total correlation matrix calculated including the correlations between ν_μ and ν_e energy bins.

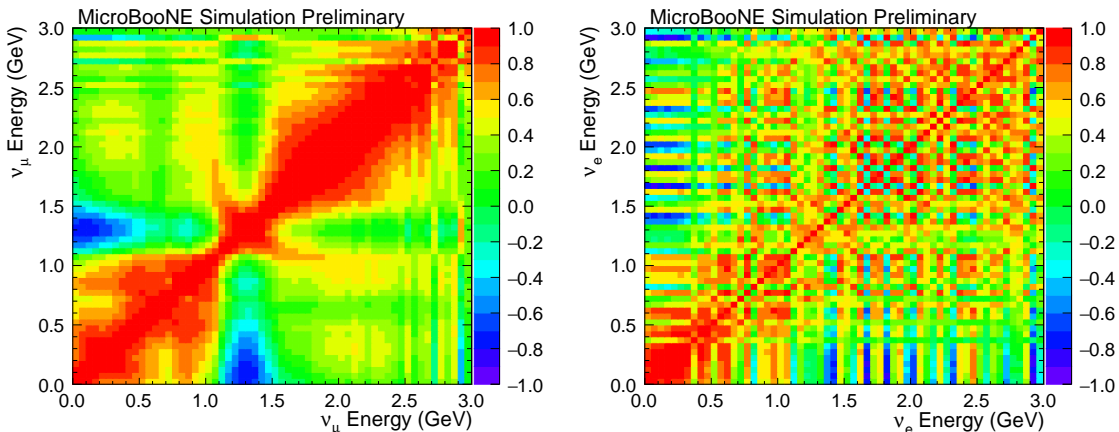


Figure 3: The total correlation matrix for ν_μ (left), and ν_e (right). The bins are in true neutrino energy.

The ν_e matrix (as well as the off-diagonal block of the $\nu_\mu - \nu_e$ matrix) is not entirely smooth due to lower MC statistics. Note that the binning shown here is finer than what is used in data analysis. Furthermore, the MC statistics used is still much higher than the

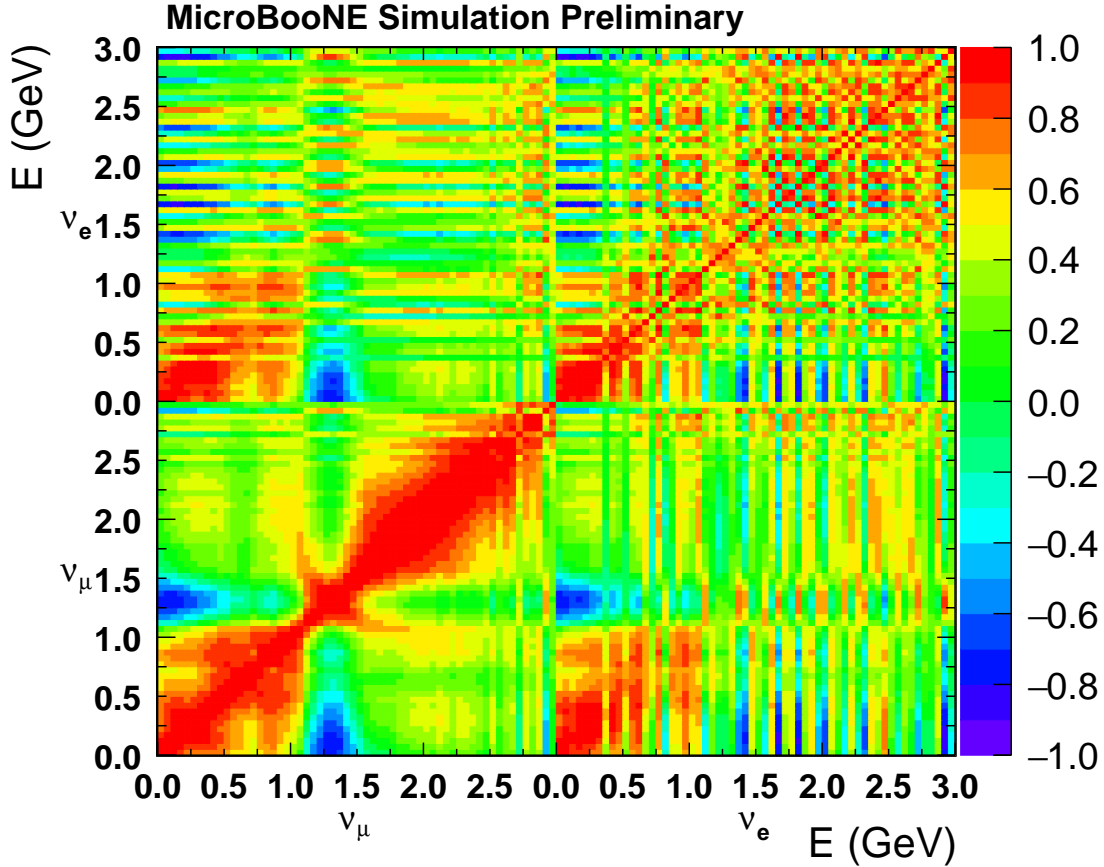


Figure 4: The total correlation matrix for ν_μ and ν_e including the off-diagonal correlations between the two neutrino species. The bins are in true neutrino energy.

expected data statistics, and therefore the noise in the off-diagonal elements of the covariance matrix will be much smaller when compared to the diagonal elements.

Table 3 shows the breakdown of systematic uncertainties on the calculated flux. The dominant uncertainties are due to hadron production uncertainties.

Figure 5 shows the fractional uncertainty on the neutrino flux, and the dominant systematics as a function of energy for each neutrino type.

A Muon neutrino flux and systematic uncertainties

Table A shows the muon neutrino flux in 50 MeV energy bins, and the associated total fractional uncertainty.

References

- [1] S. Agostinelli et al. GEANT4: A Simulation toolkit. *Nucl. Instrum. Meth.*, A506:250–303, 2003.

Systematic	$\nu_\mu/\%$	$\bar{\nu}_\mu/\%$	$\nu_e/\%$	$\bar{\nu}_e/\%$
Proton delivery	2.0	2.0	2.0	2.0
π^+	11.7	1.0	10.7	0.03
π^-	0.0	11.6	0.0	3.0
K^+	0.2	0.1	2.0	0.1
K^-	0.0	0.4	0.0	3.0
K_L^0	0.0	0.3	2.3	21.4
Other	3.9	6.6	3.2	5.3
Total	12.5	13.5	11.7	22.6

Table 1: Systematic uncertainties on the BNB flux calculation. The other category includes uncertainties in pion and nucleon total, inelastic, and quasi-elastic cross sections on beryllium and aluminum, as well as the horn current calibration uncertainty, and uncertainty in the horn current distribution. Proton delivery includes uncertainties in counting the protons on target, and the uncertainty arising from some of the protons in the tails of the beam profile not going through the whole target.

- [2] A. A. Aguilar-Arevalo et al. The Neutrino Flux prediction at MiniBooNE. *Phys. Rev.*, D79:072002, 2009.
- [3] A. A. Aguilar-Arevalo et al. First Measurement of the Muon Neutrino Charged Current Quasielastic Double Differential Cross Section. *Phys. Rev.*, D81:092005, 2010.
- [4] A. A. Aguilar-Arevalo et al. Improved Search for $\bar{\nu}_\mu \rightarrow \bar{\nu}_e$ Oscillations in the MiniBooNE Experiment. *Phys. Rev. Lett.*, 110:161801, 2013.
- [5] G. Cheng et al. Measurement of K^+ production cross section by 8 GeV protons using high energy neutrino interactions in the SciBooNE detector. *Phys. Rev.*, D84:012009, 2011.
- [6] C. Mariani, G. Cheng, J. M. Conrad, and M. H. Shaevitz. Improved Parameterization of K^+ Production in p-Be Collisions at Low Energy Using Feynman Scaling. *Phys. Rev.*, D84:114021, 2011.
- [7] E. L. Snider and G. Petrillo. LArSoft: Toolkit for Simulation, Reconstruction and Analysis of Liquid Argon TPC Neutrino Detectors. *J. Phys. Conf. Ser.*, 898(4):042057, 2017.

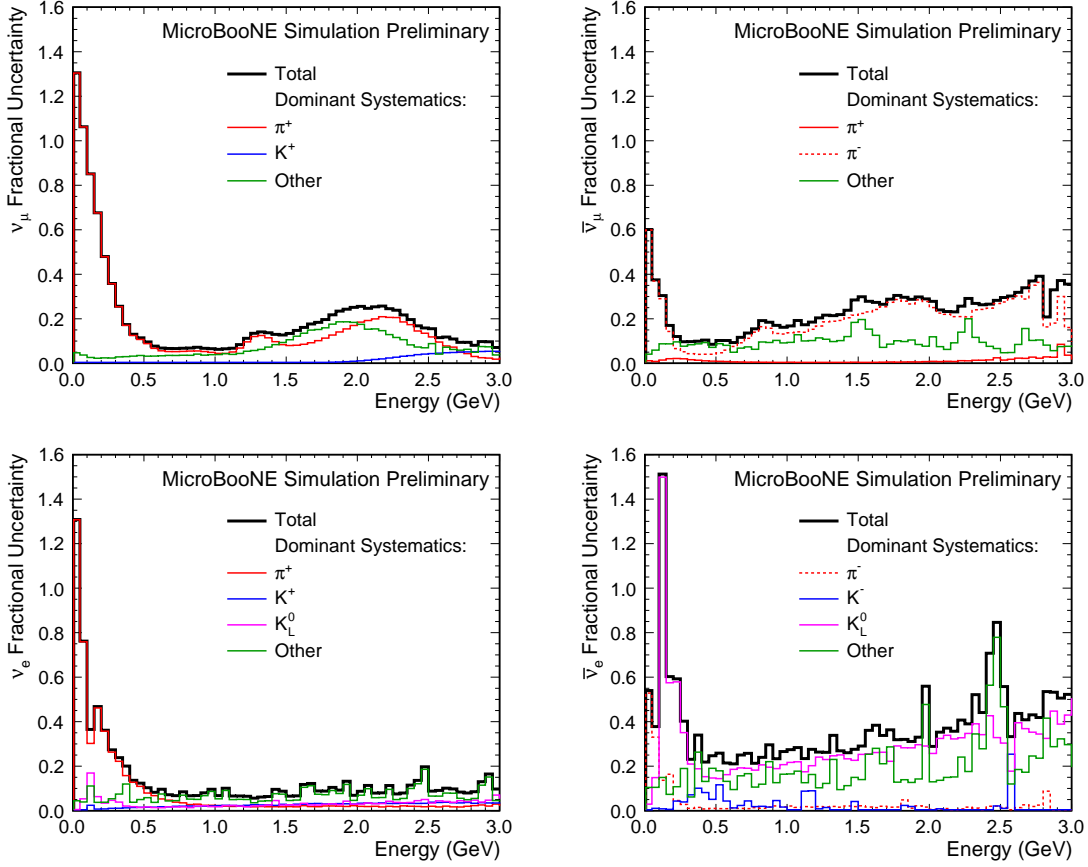


Figure 5: The total fractional systematic uncertainty for ν_μ (top left), $\bar{\nu}_\mu$ (top right), ν_e (bottom left), and $\bar{\nu}_e$ (bottom right) flux. These are the diagonal elements of the total fractional covariance matrix. Also shown are the dominant systematic contributions. The other category includes horn current miscalibration, horn current distribution mismodeling, and uncertainties due to pion and nucleon total, inelastic, and quasi-elastic cross-sections on beryllium and aluminum.

MicroBooNE Preliminary

Energy	$\nu_\mu/\text{POT}/\text{cm}^2$	Fractional uncertainty	Energy	$\nu_\mu/\text{POT}/\text{cm}^2$	Fractional uncertainty	Energy	$\nu_\mu/\text{POT}/\text{cm}^2$	Fractional uncertainty
0.00 - 0.05	3.09e-12	1.31	1.00 - 1.05	2.36e-11	0.0628	2.00 - 2.05	1.35e-12	0.256
0.05 - 0.10	1.19e-11	1.06	1.05 - 1.10	2.22e-11	0.0653	2.05 - 2.10	1.11e-12	0.247
0.10 - 0.15	1.53e-11	0.851	1.10 - 1.15	2.06e-11	0.0678	2.10 - 2.15	9.11e-13	0.254
0.15 - 0.20	1.83e-11	0.676	1.15 - 1.20	1.92e-11	0.0841	2.15 - 2.20	7.23e-13	0.257
0.20 - 0.25	2.27e-11	0.48	1.20 - 1.25	1.78e-11	0.112	2.20 - 2.25	6.21e-13	0.245
0.25 - 0.30	2.5e-11	0.359	1.25 - 1.30	1.62e-11	0.135	2.25 - 2.30	5.35e-13	0.239
0.30 - 0.35	2.67e-11	0.256	1.30 - 1.35	1.47e-11	0.141	2.30 - 2.35	4.63e-13	0.217
0.35 - 0.40	2.8e-11	0.174	1.35 - 1.40	1.32e-11	0.137	2.35 - 2.40	4.04e-13	0.197
0.40 - 0.45	2.96e-11	0.131	1.40 - 1.45	1.17e-11	0.13	2.40 - 2.45	3.67e-13	0.168
0.45 - 0.50	3.09e-11	0.115	1.45 - 1.50	1.02e-11	0.127	2.45 - 2.50	3.33e-13	0.159
0.50 - 0.55	3.16e-11	0.0961	1.50 - 1.55	8.85e-12	0.134	2.50 - 2.55	3.08e-13	0.155
0.55 - 0.60	3.16e-11	0.0773	1.55 - 1.60	7.65e-12	0.148	2.55 - 2.60	2.89e-13	0.115
0.60 - 0.65	3.12e-11	0.0686	1.60 - 1.65	6.5e-12	0.161	2.60 - 2.65	2.78e-13	0.118
0.65 - 0.70	3.09e-11	0.0667	1.65 - 1.70	5.48e-12	0.177	2.65 - 2.70	2.69e-13	0.109
0.70 - 0.75	3.06e-11	0.0663	1.70 - 1.75	4.63e-12	0.184	2.70 - 2.75	2.58e-13	0.0942
0.75 - 0.80	2.99e-11	0.0676	1.75 - 1.80	3.83e-12	0.197	2.75 - 2.80	2.4e-13	0.0943
0.80 - 0.85	2.87e-11	0.0687	1.80 - 1.85	3.18e-12	0.218	2.80 - 2.85	2.37e-13	0.0809
0.85 - 0.90	2.75e-11	0.0721	1.85 - 1.90	2.57e-12	0.235	2.85 - 2.90	2.29e-13	0.0976
0.90 - 0.95	2.63e-11	0.0674	1.90 - 1.95	2.1e-12	0.243	2.90 - 2.95	2.25e-13	0.0968
0.95 - 1.00	2.49e-11	0.0657	1.95 - 2.00	1.7e-12	0.251	2.95 - 3.00	2.09e-13	0.0711

Table 2: Muon neutrino flux through MicroBooNE TPC volume corresponding to Figure 1, and the total fractional uncertainty as shown in Figure 5.